Chapter 3

Radio Interferometric Observations: Gain Errors and Calibration

This chapter presents the systematic effects introduced during the measurement process in radio interferometric observations and discusses calibration techniques to correct these effects. These effects are commonly referred to as gain. Often the calibration process is not perfect, leaving a component of gains uncalibrated which we refer to as residual gain errors. We further study the effect of residual gain errors resulting from an error in the primary calibration on the visibilities. We have simulated the visibility for the full synthesis GMRT baseline configuration and studied the statistics of the visibilities in the presence of gain errors.

3.1 Interferometric Observation and Gain

Interferometers measure the spatial correlation of an electric field from a distant source in the sky by a pair of antennae. The spatial correlation of the measured electric field between two interferometric elements, A and B, is called the "visibility". The visibility function is directly related to the specific intensity distribution of the source in the sky by an integral

transform, given as

$$V(u,v,w) = \int_{-\infty}^{\infty}\int_{-\infty}^{\infty} A_\nu(l,m) I_\nu(l,m) e^{-2\pi i(ul+vm+wn)} \frac{dldm}{\sqrt{1-l^2-m^2}} \tag{3.1}$$

where (u, v, w) are the components of the baseline vector **U** and (l, m, n) specifies the direction cosines with respect to the phase center, associated with θ, which is a 2D-vector in the plane of the sky. $A_\nu(l,m)$ is the normalized antenna response pattern, and $I_\nu(l,m)$ is the specific intensity of the source at frequency ν.

The visibility defined in equation 3.1 represents the true sky visibility and is free from any external measurement defects. In a real observation, the visibilities measured by a pair of antennae differ from the true sky visibilities for various reasons. These include effects originating from the complex electronic chain of the instrument and the modifications introduced to the signal due to the ionosphere and other atmospheric effects. These instrumental and propagation effects are collectively known as "gain" $\mathbb{G}$, which is complex in nature. The complex instrumental response or the gain depends both on time and frequency. The observed visibility $\tilde{V}(\mathbf{U})$ is a function of baseline, and it is recorded for every pair of antennae at different frequency channels in the frequency range of observation. Note that, for a given pair of antennas, the projected antenna separation and hence the baseline vector changes with time as the antenna follows the source position in the sky.

Modern synthesis arrays operate to preserve a linear relationship between the measured visibilities and the true sky visibilities, and the measured visibilities are the true visibility multiplied by the gain. Apart from this, the recorded signal also includes measurement noise. The visibility measured at a frequency of observation ν, $\tilde{V}(\vec{U}_i)$ for the i^{th} baseline $\mathbf{U}_i$ at a time t can be given as (Hamaker et al., 1996; Taylor et al., 1999)

$$\tilde{V}(\vec{U}_i,\nu) = \tilde{\mathbb{G}}_i(t,\nu)\tilde{V}_i^S(\vec{U}_i,\nu) + \tilde{N}_i(\vec{U}_i) \tag{3.2}$$

The proportionality factor $\tilde{\mathbb{G}}_i(t,\nu)$ represents the baseline-based complex gain for the i^{th} baseline, which depends on time, frequency, and the direction of observation. $\tilde{N}_i(\vec{U}_i)$ is the stochastic noise term, which is assumed to be uncorrelated across baselines and consists mostly of thermal system noise. The noise present in the measurement process can depend on the gain as well as the total power measured by the system. The gain dependence of the noise comes from the electronics at various stages in the signal path from the receiver to the correlator. For a simplistic electronic chain of the instrument, the noise can be considered independent of the gain. The major part of the thermal noise comes from the sky temperature which is scale-dependent, due to this the noise in the image varies spatially and can be spatially correlated. Here we consider the noise in the visibility plane and represent it as a function of baseline for which these variations still need to be studied. Here $\tilde{V}_i^S$ is the visibility that would have been recorded if $\tilde{\mathbb{G}}_i(t,\nu)$ is unity and in the absence of noise. We call this the sky visibility

$$\tilde{V}_i^S = \langle \tilde{E_A} \tilde{E}_B^* \rangle \tag{3.3}$$

where E_A and E_B are the electric field signals at the dipoles of the antennas A and B.

3.1.1 Time and frequency dependence of the Gain

The complex gain $\tilde{\mathbb{G}}$ is the combined effect of telescope geometry, receiver characteristics, electronic (low noise amplifiers, filters, etc.) gain, and the ionospheric effects. The gain changes with time, frequency, and direction of observation in the sky. Variations in the environmental conditions of the receiver chain, such as temperature, etc., varying properties of the long signal path medium from the receiver to the central processing facility, etc., cause the time-variation of the gains. Gain variations over time also arise from the ionospheric and atmospheric properties, which change rapidly with time and direction. The

atmospheric (Ionosphere and troposphere) turbulence profoundly affects electromagnetic wave propagation. The ionospheric turbulence (mostly the charged particles and ions) adds to the low-frequency electromagnetic radiation's phase distortions. The water vapors present in the troposphere also degrade interferometric observations. While tracking the source, as the antenna looks through a different patch of sky, it sees a different part of the ionosphere and troposphere. This results in the direction dependence of the gains, including the antennae's primary beam response. Azimuthal rotation of the alt-azimuth mount telescopes results in time-dependent antenna primary beam patterns. Antenna pointing errors resulting from the deformations caused by the gravity loading of the antenna, wind loading, etc., give the time and direction-dependent antenna gains.

Antenna gain properties also vary with the frequency of observation. The spectral dependence of the gain primarily comes from the bandpass filter properties of the receiver. The electronic properties/response of the receiver chain, filters, and amplifiers strongly depend on the frequency. With the complex antenna electronics, atmospheric properties also vary slightly with frequency and contribute to the frequency-dependent gain. The frequency-dependent part of the gains varies slowly with time, but usually, they are assumed to be time-independent; hence, they are treated independently from the time-dependent gains and collectively termed as bandpass.

The electric field of an electromagnetic wave originating from a source in the sky suffers several modifications before it is recorded. These include the influence of the ionosphere, the geometrical properties of the antenna and receivers, and several amplifiers used in the signal chain. In this work, we are considering a rather simple view, where a single multiplicative complex gain encapsulates all the above effects. We shall consider the real and imaginary parts or the amplitude and phase parts of these gains in calculations. Further, for simplicity, we will further take the real/imaginary or amplitude/phase parts of the residual gains to be uncorrelated. Note that this assumption is not well justified in

an actual telescope. The correlation between the real/imaginary or amplitude/phase parts will give rise to additional effects than discussed here and will be addressed separately in future work.

3.1.2 Decomposing the complex gain into antenna-based gains

The baseline-based complex gain $\tilde{\mathbb{G}}_i(t,\nu)$ in each visibility arises from the individual gains of the antenna pairs used to estimate it. Along with the time and frequency, it also depends upon the direction of observation, though we assume it here to be direction independent. The instrument's frequency response varies slowly with time, but it can be assumed to be time-independent. Under this assumption, we can write the time and frequency-dependent part of the gain separately as

$$\tilde{\mathbb{G}}_i(t,\nu) = \mathrm{G}_i(t)\tilde{\mathfrak{B}}_i(\nu) \tag{3.4}$$

Here $\mathrm{G}_i(t)$ represents the time-dependent component of the gain or just gain, and the frequency-dependent part of the gain $\tilde{\mathfrak{B}}_i(\nu)$ is known as the bandpass. The index i in each case denotes that the quantities are specified for the i^{th} baseline. Hereafter, we shall refer to the time-dependent part of the gain $\mathrm{G}(t)$ as "gain" and frequency dependent part of the gain $\tilde{\mathfrak{B}}_i(\nu)$ as "bandpass".

As the visibility measurements involve a pair of antennae, the baseline-based gains arise from the individual gains of the pair of antennae involved in the visibility measurements. If the digital correlator doesn't produce any error in correlation, and all the effects are due to antennae or transmission lines, only then we can write the baseline-based gains in terms of antenna-based gains as

$$\tilde{\mathrm{G}}_i(t) = \langle \tilde{g}_A(t)\tilde{g}_B^*(t)\rangle, \tag{3.5}$$

Similarly, for the bandpass, we can write

$$\tilde{\mathfrak{B}}_i(\nu) = \langle \tilde{b}_A(\nu)\tilde{b}_B^*(\nu)\rangle. \tag{3.6}$$

where $\tilde{g}_A(t)$, $\tilde{g}_B(t)$ and $\tilde{b}_A(\nu)$, $\tilde{b}_B(\nu)$ are the gain and bandpass response of the individual antenna A and B respectively; angle brackets represent the average over the integration time.

3.2 Calibration

As discussed above, in interferometric visibilities, there always exist effects introduced by the atmosphere (e.g., troposphere and ionosphere) and the instrument (e.g., beam shape, frequency response, receiver gains, etc.). Apart from this, some random high-intensity signals can be present in the data, which is known as Radio Frequency Interference (RFI). These RFIs usually do not affect the full observation but can be present only for a particular time, frequency channel, or antenna. This may not be present in both polarizations of the signal as well. These systematics must be known and corrected before using the observed visibilities for any scientific purpose. The process of estimating and correcting the errors in these measurements is called calibration and is an essential step before understanding the measured data.

Various calibration strategies are discussed in the literature to correct for the time, frequency, and direction-dependent gains. These include observation of the standard calibrator sources to measure long-time scale variation of the gain known as primary calibration, self-calibration (Pearson and Readhead, 1984) to reduce the effect of rapid ionospheric changes, redundancy calibration (Noordam and de Bruyn, 1982; Wieringa, 1992), etc. For the telescopes with a large field of view, additionally, direction-dependent calibration techniques are used to estimate and mitigate the effect of the ionosphere along

with different directions over each antenna (van der Tol et al., 2007; Wijnholds and van der Veen, 2009).

We usually solve the complex gain $\mathbb{G}_i(t,\nu)$, defined in equation 3.2, for each channel separately which essentially gives us the time-dependent gain solution $\mathrm{G}_i(t)$. The instrument's frequency response is later corrected separately with the help of standard bandpass calibrator sources. For single channel observation the measurement equation 3.2 can be given as

$$\tilde{V}(\vec{U}_i) = \tilde{\mathrm{G}}_i(t)\tilde{V}_i^S(\vec{U}_i) + \tilde{N}_i(\vec{U}_i) \tag{3.7}$$

The baseline-based complex gain $\tilde{\mathrm{G}}_i(t)$ can approximate by the product of two associated antenna-based complex gains $\tilde{g}_A(t)$ and $\tilde{g}_B(t)$ as given in equation 3.5. In calibrating the gain, it is best to consider the amplitude and phase separately, since the errors in these two quantities generally arise through different mechanisms. For example, atmospheric fluctuations cause phase fluctuations but have little effect on the amplitudes. So we can write the antenna-based complex gains for antennae A and B in terms of the amplitudes and phases of the antenna A and B as

$$\tilde{g}_A(t) = a_A(t)e^{i\phi_A(t)}\ ; \qquad \tilde{g}_B(t) = a_B(t)e^{i\phi_B(t)} \tag{3.8}$$

where $a_A(t)$ is an antenna-based amplitude correction and $\phi_A(t)$ is the antenna-based phase correction, similarly, the quantities with subscript B denote the same for antenna A. To calibrate the time-dependent complex gain $\tilde{\mathrm{G}}_i(t)$ an unresolved calibrator source can be observed keeping it at the center of the field of view of observation. If S_c is the flux density of the calibrator source, the measured response of the instrument can be given as

$$\tilde{V}_c(\mathbf{U}_i) = \tilde{\mathrm{G}}_i(t)S_c \tag{3.9}$$

Here subscript c denotes the calibrator. With the help of the above equation, we can get the gain $G_i(t)$ which will be

$$\tilde{G}_i(t) = \frac{\tilde{V}_c(\mathbf{U}_i)}{S_c} \tag{3.10}$$

his gain $G_i(t)$ can be used to get the calibrated visibilities. From the baseline-based gains $G_i(t)$ obtained above we get the antenna-based gain $\tilde{g}_A(t)$. To get the baseline-based gains $G_i(t)$, one needs to solve for ${}^NC_2$ complex numbers, and the presence of noise in each visibility measurement often makes it difficult to get the accurate baseline-based gains after the calibration. Decomposing the baseline-based gain into the antenna-based gain consequently reduces the total unknown complex gains, from ${}^NC_2$ to N. Usually, for an N-element interferometer, the number of baselines will be far more than the elements, and solving for antenna-based gain becomes an overly determined system of equations.

The calibrator source is observed at regular intervals during the whole observation, giving the amplitude and phase gain solutions as a function of time. The gain values are then interpolated to the time when the target source was observed. The time-dependent gain has slowly varying instrumental and rapidly varying ionospheric components. The temporal and spatial variation of the atmospheric effects may cause the actual values of the $\tilde{G}_i(t)$ to be different for the target source from the one obtained from the calibrator, leaving some residual gain errors in the gain solutions. In some cases, we may also not have a bright source nearby the target. The errors induced because of these are later corrected using what is known as "self-calibration". In this procedure, the time-series antenna gain solutions are obtained iteratively, using the rough image of the target source itself as a model and calibrating the data. First, a model is constructed using the primarily calibrated data of the target source; using this model, the complex gains are solved, and gain solutions are applied to the source. This process is repeated iteratively unless stable gain solutions are obtained and no further improvement in the source is seen. As discussed above, the complex gain also depends upon the frequency. The frequency-dependent part

of the gain $\mathfrak{B}_i(\nu)$ is solved by the process called bandpass calibration. Good bandpass calibration is key to detecting and accurately measuring spectral features, especially weak, broad features. Bandpass calibration can also be the limiting factor in a dynamic range of continuum observations. Direction-dependent effects, which include the direction of propagation of the signals, the primary beams of the antennas, the effects of the ionosphere and troposphere, etc., require observing many calibrator sources in different directions near the target source.

3.2.1 Errors in the Calibration

In the previous sections, we discussed the systematic effects present in the observation and the various calibration techniques to correct these effects. Obtaining the exact gain solutions is very difficult, and even after investing a good amount of effort in the calibration and data reduction, there remain some residual effects, which limit the accuracy of the gain solutions. There are various reasons which lead to the origin of residual gain errors. Some of these are the rapidly fluctuating ionosphere, the presence of thermal noise in the visibilities, uncertainties in the sky models, unwanted RFI signals, complicated instrumental effects, etc.

Primary calibration is done by observing a calibrator source and using this we solve for the gains of the antenna. For good calibration, the calibrator source should have a few properties like it should be a bright unresolved source of known intensity and position, also it should be near the source. Error in the intensity and position of the calibrator will lead to the erroneous estimate of time-varying amplitude and phase gains. The absence of a bright calibrator near the target source also limits the accuracy of the calibration. During the observation, if the calibrator source is away from the target source, then using it as a calibrator may leave us with some uncalibrated directional effects, as the directional properties of the medium for the calibrator and target source would be completely different.

The source of gain errors also includes the antenna pointing inaccuracy, error in the antenna positions, the difference in antenna primary beam, and change in the electronic; the former two lead to some residual phase errors, while the latter may introduce both amplitude and phase errors. Similarly, one needs to observe the bright flat spectrum source with no spectral feature for Bandpass calibration. Often it is very difficult to find such sources in the sky during the observation. This will give frequency-dependent residual gain errors. Rapid fluctuations in the bandpass make it difficult to model the gain and add to the frequency-dependent gain errors.

The time and frequency-dependent residual gain errors are also expected to be correlated. As antennae track the source in the sky, the beam pattern of the antennae rotates in the sky; small asymmetry in the antenna beam pattern, parallactic angle rotation, and time coherence in the electron density variation in the ionosphere are expected to introduce time correlation in the residual gains. In case of any missing channels due to RFI or bad instrumental response, the bandpass gain solution is interpolated between the channels or modeled using a polynomial function. This leads to frequency-correlated gains, and errors in the bandpass will result in frequency-correlated residual gain errors.

The calibration errors associated with an incomplete sky model affect redundant calibration even in the case of perfect redundancy and identical antenna beams, and these errors can exceed the predicted EoR signal (Byrne et al., 2019). In the case of redundancy calibration, errors in gain solutions are also introduced due to the non-redundancy of the arrays. Liu et al. (2010) shows that non-redundant baseline distributions result in spectral structures contaminating the EoR detections. Dillon et al. (2020) have also studied the effect of non-redundancy on the gain solutions for a redundant array such as HERA. This introduces characteristic patterns into the gain solutions, affecting the calibrated visibilities and power spectra. Joseph et al. (2018) investigated the effect of sky flux distribution and antenna position offsets in redundancy calibration. The position offsets introduce a

bias into the complex gain solutions phase. They notice an enhancement in the bias as the distance between bright radio sources and the pointing center and the flux density of the sources increases. The deviations from perfect redundancy due to the antenna-to-antenna variations in redundant-baseline calibration produce considerable foreground power leakage from the wedge contaminating a considerable fraction of the EoR window (Orosz et al., 2019). The effect of primary beam non-redundancy using simulations is also studied in Choudhuri et al. (2021). They find that an additional temporal structure is induced in the gain solutions. Usually, the calibration errors are relatively small, and the residual gain errors can be neglected for the bulk of the interferometric observations. However, accurate calibration of instrumental effects is much needed for high dynamic range observations such as the redshifted 21-cm signal in the presence of bright foreground. We investigate the effect of calibration inaccuracy by modeling the statistics of residual gain errors without referring to a particular mechanism that may lead to it. Furthermore, the residual gain errors can significantly contribute to the uncertainty in the power spectrum measurements.

In the process of self-calibration, sky models are used to estimate the gains. Since the sky models are estimated from the same observed visibilities, in the initial phases of the self-calibration the errors in the estimated gains arise partly because of the improper estimate of the sky, and hence the gain errors are correlated with the sky model. As the self-calibration steps proceed the sky model inaccuracy reduces and the correlation of the residual gain errors with the sky model also reduces. Hence, in the case of high dynamic range observations, it is much more important to have a proper model of the strong part of the sky to avoid improper gain estimations. In this work, we assume that a proper model for the foreground exists and hence the residual gain errors are not correlated with the foreground sky.

3.3 Residual Gain Errors and Its Effects

The visibilities are calibrated for the complex gains and prepared for further analysis. After the calibration, one should have the observed visibility as the true visibility, but the calibration process can be erroneous for various reasons and can give inaccurate gain solutions. For the purpose of our work, we assume that the best calibration procedure for the data in consideration has been performed and applied. In principle, after calibration, the gain amplitude should be one, and the phase should be zero. Still, as discussed, it deviated from its principal value for numerous reasons leaving some uncorrected components of gain. Here we refer to the uncalibrated part of the gain as residual gain errors (or residual gains). In this work, we study the effect of residual gain errors in primary calibration. Here we assume a simple gain error model and study its effect on observed visibilities by considering a single point source at the phase center.

3.3.1 Analytical Results

At the end of the calibration step, calibration is done, and only the residual gains for each antenna contribute to the gain term $\tilde{G}_i(t)$. Hence, at this stage, we can write the antenna-based gains $\tilde{g}_A(t)$ and $\tilde{g}_B(t)$ as

$$\begin{aligned} \tilde{g}_A(t) &= (1+\delta_A(t))e^{i\phi_A(t)}, \\ \tilde{g}_B(t) &= (1+\delta_B(t))e^{i\phi_B(t)} \end{aligned} \tag{3.11}$$

where $\delta_A(t)$ and $\phi_A(t)$ are the residual amplitude gain error and the residual phase gain error respectively for antenna A. After the calibration is done, these residual gain errors are expected to be small compared to unity. Here we model the residual gain errors as time-independent Gaussian random variables with zero mean and quantify them with the

following properties

$$\langle \delta_A(t) \rangle = \langle \delta_B(t) \rangle = 0 \; ; \;\; \langle \delta_A(t) \delta_B(t') \rangle = \delta_{AB} \sigma_\delta^2 \delta_D(t-t'),$$
$$\langle \phi_A(t) \rangle = \langle \phi_B(t) \rangle = 0 \; ; \;\; \langle \phi_A(t) \phi_B(t') \rangle = \delta_{AB} \sigma_\phi^2 \delta_D(t-t')$$

σ_δ^2 and σ_ϕ^2 being the variance of the residual amplitude and phase gain errors, and δ_D is the Dirac delta function. There is no correlation between the amplitude and phase of the gain errors, also no cross-antenna correlation in the gains is considered. Here we do not consider any frequency dependence of the gain. The visibility measured by a pair of antennae A and B, in terms of antenna-based gains, after calibration can be written as

$$\tilde{V}_{AB}(t) = g_A(t) g_B^*(t) V_{AB}^S = \langle (1+\delta_A(t))(1+\delta_B(t)) e^{i(\phi_A(t)-\phi_B(t))} \rangle \tag{3.12}$$

where V_{AB}^S is the sky visibility. We do not consider the thermal noise here. The thermal noise is assumed to be a Gaussian Random variable, the effect of the thermal noise then can be reduced by increasing the total observation time. Visibility is generally a complex quantity, we can write it in terms of real and imaginary parts as

$$\begin{aligned} \tilde{V}_{AB}(t) &= V_R + iV_I \\ V_{AB}^S &= V_r + iV_i \end{aligned} \tag{3.13}$$

Using this decomposition in equation 3.12 and solving for we get

$$\begin{aligned} V_R &= \langle (1+\delta_A(t))(1+\delta_B(t)) \rangle [\langle Cos(\phi_A - \phi_B) \rangle V_r - \langle Sin(\phi_A - \phi_B) \rangle V_i] \\ V_I &= \langle (1+\delta_A(t))(1+\delta_B(t)) \rangle [\langle Sin(\phi_A - \phi_B) \rangle V_r + \langle Cos(\phi_A - \phi_B) \rangle V_i] \end{aligned} \tag{3.14}$$

As the gain errors are small, we can expand sin and cos terms in series and neglect third and higher-order terms. Under these approximations and using the properties of the gain

errors defined in 3.12 the real and imaginary components of measured visibility is

$$V_R = (1-\sigma_\phi^2)V_r,$$
$$V_I = (1-\sigma_\phi^2)V_i \tag{3.15}$$

Similarly, we can solve for the uncertainties in the real and imaginary parts of the measured visibility. The uncertainties in real and imaginary part of the visibility σ_R^2 and σ_I^2 is

$$\sigma_R^2 = \langle V_R^2\rangle - \langle V_R\rangle^2 = 2[\sigma_\delta^2 V_r^2 + \sigma_\phi^2 V_i^2]$$
$$\sigma_I^2 = \langle V_I^2\rangle - \langle V_I\rangle^2 = 2[\sigma_\phi^2 V_r^2 + \sigma_\delta^2 V_i^2] \tag{3.16}$$

Equations 3.15 and 3.16 show the effect of residual gain errors on the amplitude and uncertainties of the real and imaginary part of the measured visibility, respectively.
The primary calibration is done by observing a bright point source keeping the source at the phase center while observing. For a source with a given specific intensity I_ν at phase center its visibility will have only real component i.e. $V_i = 0$ and hence $V_{AB}(t) = V_r$. So the measured visibility after calibration would be

$$V_R = (1-\sigma_\phi^2)V_r\ ;\ \ V_I = 0$$
$$\sigma_R^2 = 2\sigma_\delta^2\ ;\ \ \sigma_I^2 = 2\sigma_\phi^2 \tag{3.17}$$

3.3.2 Simulation Results

Giant Meter-wave Radio Telescope (GMRT) is operated by NCRA-TIFR, Pune, situated in Narayan Gaon, Khodad (80 km east of Pune) and is one of the most sensitive radio telescopes in the world (Swarup, 1991). It has 30 parabolic antenna dishes, with each antenna dish having a diameter of 45 m. Dishes are arranged in Y-shape, and the largest

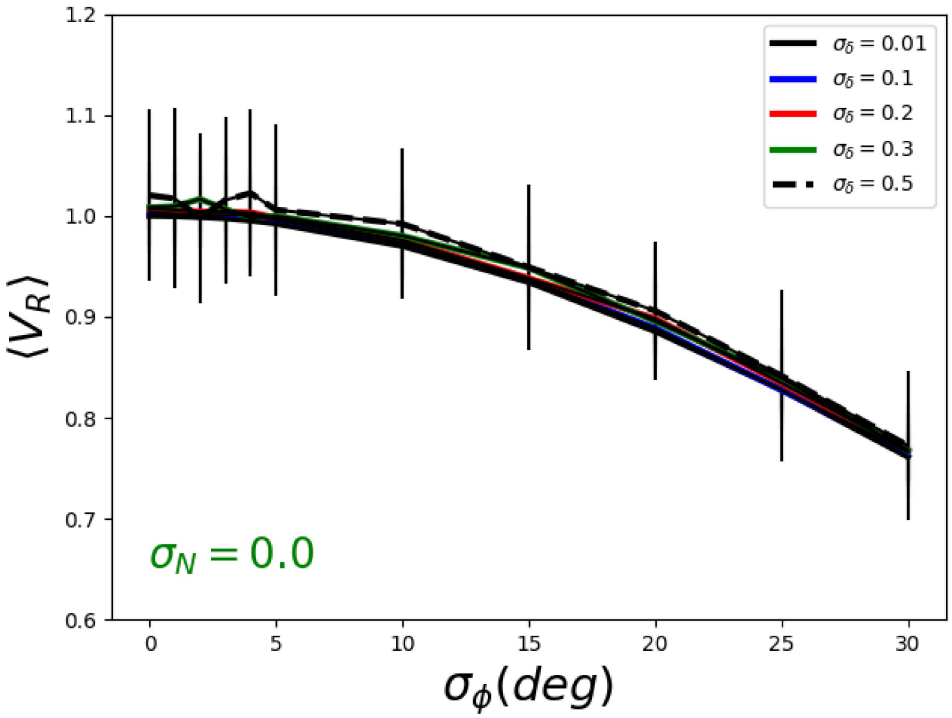

Fig. 3.1 Variation of the real part of the visibility with residual phase gain error for different amounts of residual amplitude gain errors σ_δ.

baseline of the interferometer is approximately 25 km giving a resolution of around 20 arc-second at 150 MHz. We simulate visibilities for the GMRT baseline configuration for 8 hours of observation time with a single point source of known intensity and position. Here we have taken the strength of the source to be unity. This will give the real component of the sky visibility to be one, and the imaginary component will be zero. We have simulated the visibilities for this source in the presence of the gain errors based on the gain error model given by equation 3.12. We have varied the number of gain errors and checked the statistics of the simulated visibilities to see the effect of amplitude and phase gain errors.

In figure 3.1 we have plotted the mean of the real component of the visibility $\langle V_R \rangle$ with the antenna-based phase gain error σ_ϕ for different values of antenna-based amplitude gain error σ_δ. Here we found that with an increasing amount of phase gain error σ_ϕ, the amplitude of visibility decreases, which is in agreement with our analytical results (see

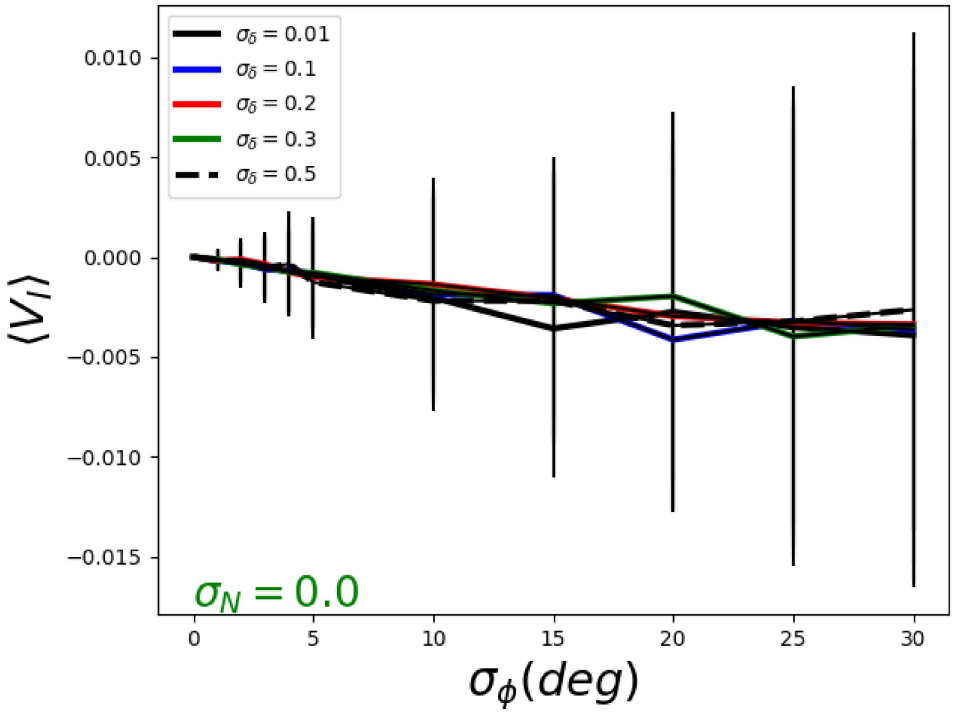

Fig. 3.2 Variation of the imaginary part of the visibility with phase gain error for different amounts of residual amplitude gain errors σ_δ.

equation 3.17). Figure 3.2 shows the variation of the mean of the imaginary part of the visibility $\langle V_I \rangle$ with σ_ϕ. We see that mean of the imaginary part of the visibility $\langle V_I \rangle$ is almost zero. Here we find that initially, it is zero (which is because of the fact that for a point source at the phase center, the imaginary part of the visibility is zero), but as phase gain error σ_ϕ increases, $\langle V_I \rangle$ starts becomes slightly negative. This effect is mostly due to the higher-order terms in σ_ϕ we have neglected. The bars in these two figures show the uncertainty level of visibility.

We check the effect of amplitude gain error σ_δ on the amplitude of the visibility, but we found no significant change in the amplitude of the visibility. From these figures, we find that the effect of the phase gain error is to reduce the amplitude of the visibility. Our analytical calculations (equation 3.15 and 3.17) also indicate the same behavior

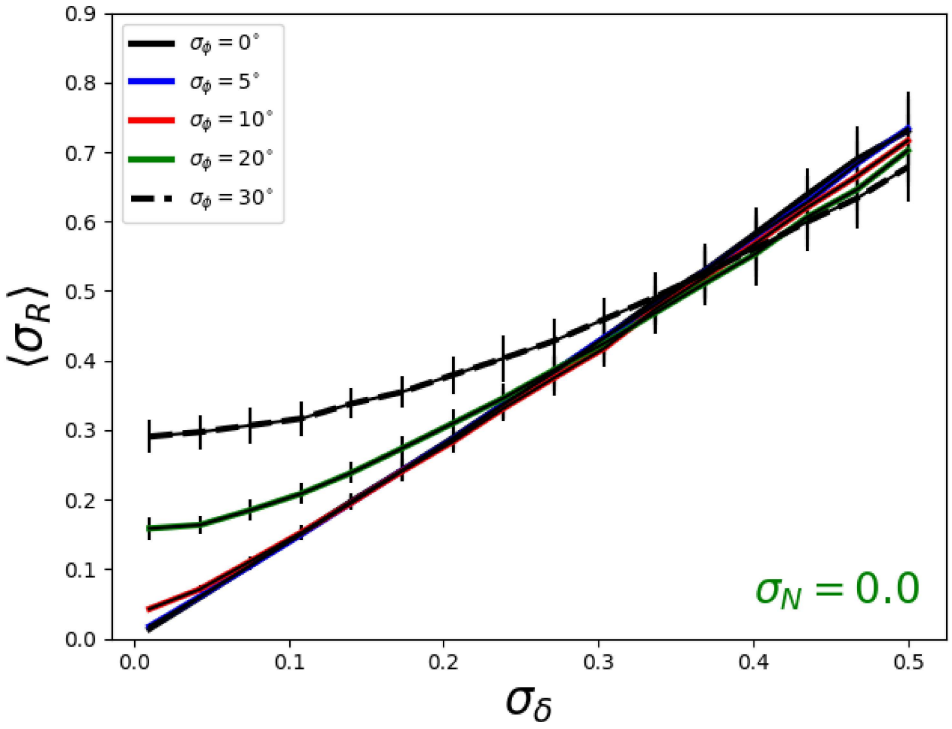

Fig. 3.3 Effect of amplitude gain error on the noise in the real part of visibility for various residual phase gain errors σ_ϕ.

of decrement in the amplitude of visibility with phase error σ_ϕ and unaffected by the amplitude gain error σ_δ and hence verified by the simulation results.

We study the statistics of the uncertainties in visibility because of the residual gain errors after calibration.In figure 3.3 we plot the noise in the real part of the visibility σ_R against the amplitude gain error σ_δ for different values of phase gain error σ_ϕ, we found that noise in the real part of the visibility σ_R increases with increase in the amplitude gain error σ_δ. In figure 3.4 we show the noise in the imaginary part of the visibility σ_I against the phase gain error σ_ϕ, and we found the same behavior.

In figure 3.3 we see a slight change in the behavior of the curves with higher σ_ϕ values like σ_ϕ = 20° or 30°, and they become lower compared to that with low σ_ϕ value like 0° or 5° at higher-end that is because that for higher σ_ϕ values the fourth-order terms that we have neglected in the calculation starts contributing and they effectively decreases

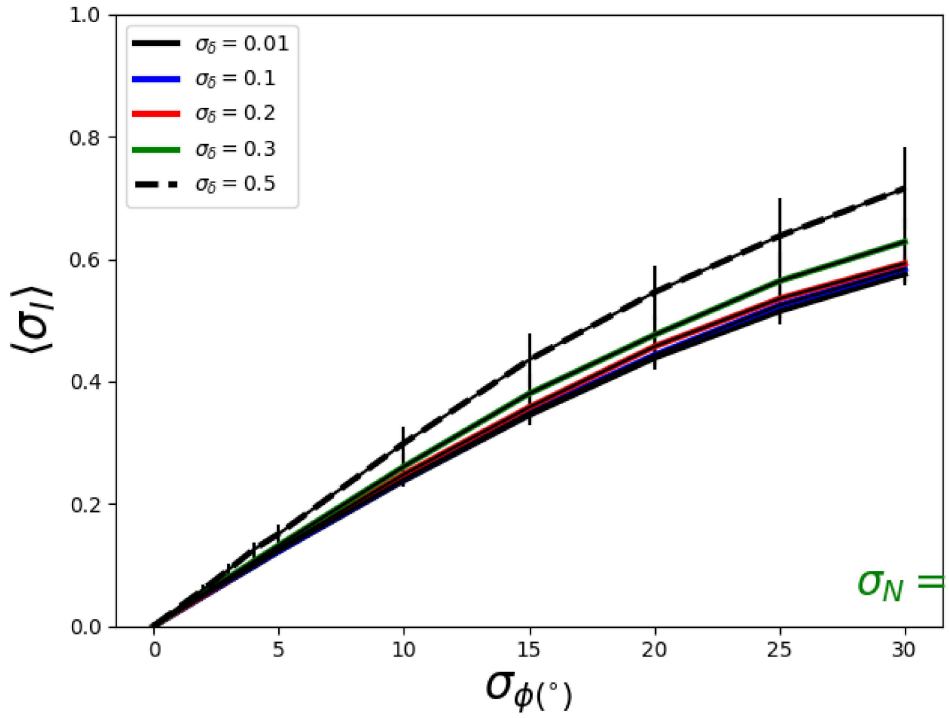

Fig. 3.4 Effect of phase gain error on the noise in the imaginary part of visibility for various residual amplitude gain errors σ_δ.

the noise. Similarly, in figure 3.4 we see that the curves with different σ_δ values start separating from each other, and the one with high σ_δ value shifts towards the upper side that is, again, because of the higher-order terms (like cross term $\sigma_\delta^2\sigma_\phi^2$ in this case). This effectively increases the noise in the visibility, which we have neglected in the analytical calculation.

3.3.3 Discussion and Conclusion

In this chapter, we consider the actual interferometric observation and discuss various systematic effects present in the measurement process and methods to resolve them. We studied the effect of residual gain errors in primary calibration analytically and using simulations. Here we do not include thermal noise in our study. The highlights of this chapter are the following

- In actual observations, the sky visibilities are modified due to the presence of various instrumental and ionospheric effects, collectively termed as gain. These systematics often depend on the time, frequency, and direction of observation. Various techniques such as primary calibration, self-calibration, bandpass calibration, etc., are used to solve for the time and frequency-dependent gains.

- Due to various practical reasons, the calibration process is not perfect, and this leaves a component of gains uncalibrated. The uncorrected part of the gain is referred to as the residual gain errors. These residual gains are often correlated in time and frequency.

- We further discuss a case of a single point source in the presence of residual gain error. Using the statistics of visibilities, we demonstrate how the uncorrected gain errors affect the calibrated visibilities.

- The presence of residual gain errors results in the reduction of the real and imaginary components of the visibility amplitudes. Further, it enhances the uncertainties in the visibility measurements.

This shows that if our primary calibration is not perfect, this will affect the visibility statistics, affecting further observation analysis. The effect of these gain errors is small for the observation of bright sources, but for the detection of weaker signals like the EoR 21-cm signal, where a high dynamic range is required, these errors accompanied by the bright foreground can be significant, and make the detection even more challenging.

****